Reprinted from JOURNAL OF APPLIED PHYSICS, Vol. 37, No. 9, 3594–3598, August 1966
Copyright 1966 by the American Institute of Physics
Printed in U. S. A.

Eddy-Current-Limited Domain-Wall Motion in Thin Ferromagnetic Films

CARL E. PATTON, THOMAS C. MCGILL,* AND CHARLES H. WILTS
California Institute of Technology, Pasadena, California
(Received 9 March 1966; in final form 2 May 1966)

The effect of eddy current losses on domain-wall motion in thin ferromagnetic films has been investigated from a theoretical point of view. Earlier calculations neglecting wall shapes and stray demagnetizing fields do not adequately explain existing experimental data. A general expression has been developed for the current distribution about a moving Bloch wall of arbitrary shape in a thin film of infinite extent and arbitrary thickness. Stray demagnetizing field effects have been included in an approximate manner for a simple 180° wall in which the magnetization rotates linearly through a wall whose width is calculated from static energy considerations. The current distribution was evaluated numerically and the eddy-current-limited wall mobility was obtained as a function of film thickness from 400 to 4000 Å, using material parameters typical for Ni–Fe alloy films with 80% Ni. Although the current distributions exhibited a significant dependence on wall width, the mobilities were not significantly different from previous predictions. In order to explain existing mobility data on the basis of eddy current losses, wall widths much larger than calculated static Bloch wall widths must be assumed. Otherwise, some other loss mechanism must dominate.

INTRODUCTION

THE limitation of domain-wall velocities in ferromagnetic thin films has been ascribed to two mechanisms, intrinsic damping and eddy current losses. Intrinsic damping, which may be viewed as direct energy transfer to the crystal lattice by spin-wave generation of phonons, can be treated in a phenomenological manner, as developed by Landau and Lifshitz.[1] The effect of eddy current losses has been treated analytically by Williams *et al.*[2] (WSK). Several experimental investigations have been reported which undertake to characterize wall motion in terms of one loss mechanism or the other. Menyuk[3] carried out flux reversal measurements using Permalloy tape cores varying in thickness from $\frac{1}{8}$ to 1 mil and concluded that for $\frac{1}{8}$-mil thickness the eddy current losses predicted by WSK contributed only 10% to the measured wall mobilities. On the basis of these data, intrinsic damping may be presumed to be the mechanism limiting wall mobility for film thick-

* This work was done during the tenure of a National Science Foundation Graduate Fellowship.
[1] L. Landau and E. Lifshitz, Physik Z. Sowjetunion **8**, 153 (1935).
[2] H. J. Williams, W. Shockley, and C. Kittel, Phys. Rev. **80**, 1090 (1950).
[3] N. Menyuk, J. Appl. Phys. **26**, 692 (1955).

ness less than 30 000 Å. Ford,[4] on the other hand, reached a different conclusion using Kerr-effect domain-wall velocity measurements for nickel–iron films with thicknesses between 700 and 4000 Å. He observed a thickness dependence for the mobility which was inconsistent with the intrinsic damping mechanism but was consistent with the WSK calculation except that all values were lower than the calculated mobilities by a factor of about 1.7. On this basis, Ford concluded that eddy current losses were the dominant loss mechanism even for films as thin as 700 Å. Recent mobility measurements by Patton and Humphrey,[5] and Middelhoek[6] in the 1000–2000-Å thickness range were at variance with Ford's result and indicated that eddy current losses predicted by WSK contributed only about 15% to the mobility, with the remainder (85%) to be attributed to intrinsic losses.

In light of this situation, it seems desirable to examine the eddy current losses in more detail to be sure that the approximations of the WSK solution do not introduce errors which have a significant effect on the calculated mobility. In the WSK calculation, the domain wall is represented by a transition region of zero width. For this situation, the eddy current components decrease almost exponentially with distance from the transition region with decay lengths which are roughly equal to known wall widths.[7] If the current distribution extended for distances large compared to the wall width, the actual wall shape would be expected to have very little effect on the losses associated with the eddy currents. However, since the currents extend only for distances comparable to wall widths, the effect of the nonzero wall width might significantly alter the loss calculation. The present treatment improves the WSK calculation in two ways. In order to determine the effect of nonzero wall width on the eddy currents, a general expression was developed for the current distribution about a moving Bloch wall of arbitrary shape in a thin film of infinite extent and arbitrary thickness. Furthermore, for very thin films, the nonzero divergence of the magnetization at the film surfaces in the vicinity of the wall gives rise to a demagnetizing field $\mathbf{H}_s$. The effect of this stray demagnetizing field on the eddy current distribution was included in an approximate way using the stray field calculation developed by Middelhoek.[7] With these modifications, the effect of eddy current losses on domain wall velocity was evaluated numerically for a simple wall shape in which $\mathbf{M}$, the magnetization, rotates linearly with distance through a wall between antiparallel domains. The distance over which the rotation of 180° occurs is called the wall width a. The moving linear wall is assumed to have a width equal to that calculated by Middelhoek[7] for a stationary wall.

[4] N. C. Ford, Jr., J. Appl. Phys. **31**, 300S (1960).
[5] C. E. Patton and F. B. Humphrey, J. Appl. Phys. **37**, 1270 (1966).
[6] S. Middelhoek (private communication).
[7] S. Middelhoek, thesis, University of Amsterdam, Holland, 1961.

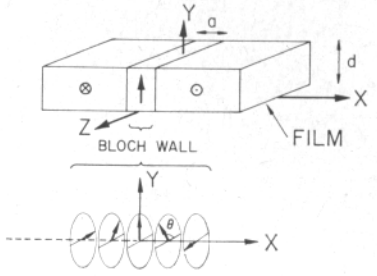

FIG. 1. Film geometry and Bloch-wall orientation where d is the film thickness and a is the wall width.

EDDY CURRENT SOLUTION

Assuming no charge separation and neglecting displacement currents in a conducting medium, Maxwell's equations may be written

$$\nabla\cdot\mathbf{J}=0, \tag{1a}$$

$$\nabla\times\mathbf{H}=(4\pi/c)\mathbf{J}, \tag{1b}$$

$$\nabla\times\mathbf{J}=-(\sigma/c)(\partial/\partial t)(\mathbf{H}+4\pi\mathbf{M}), \tag{1c}$$

$$\nabla\cdot\mathbf{B}=0, \tag{1d}$$

where the current density $\mathbf{J}$ is equal to the conductivity σ multiplied by the electric field. The magnetic induction $\mathbf{B}$ equals $\mathbf{H}+4\pi\mathbf{M}$, where $\mathbf{H}$ is the magnetic field and $\mathbf{M}$ is the magnetization. Gaussian units are employed throughout.

If $\mathbf{H}$ is assumed small compared to $4\pi\mathbf{M}$ in a ferromagnetic thin film, Eqs. (1a) and (1c), together with proper boundary conditions, can be used to obtain solutions for $\mathbf{J}$ within the film. This solution for $\mathbf{J}$, as obtained in the following discussion, and Eq. (1b) can then be used to verify the initial assumption that $H\ll 4\pi M$ for the fields produced by the eddy currents. As calculated by Middelhoek,[7] the stray demagnetizing field, associated with Bloch walls, is not necessarily small compared to M. This field will be included, in an approximate manner, for the specific case of a linear wall. The film and wall geometry are shown in Fig. 1. As shown in this figure, the magnetization orientation within the wall is denoted by θ, with $\theta=0$ at $x=-\infty$ and $\theta=\pi$ at $x=+\infty$. The film is assumed to have infinite extension in the x and z directions, the magnetization orientation is assumed to be a function of x only, and $\partial\mathbf{J}/\partial z$ is assumed zero. The calculation is carried out for a single isolated domain wall.

In Eq. (1c), the time derivative can be replaced by $v\partial/\partial x$ if the wall has a steady-state shape and a velocity v. The following differential equations for J_x, J_y, and J_z result:

$$(\partial^2 J_x/\partial x^2)+(\partial^2 J_x/\partial y^2)=0, \tag{2a}$$

$$(\partial^2 J_y/\partial x^2)+(\partial^2 J_y/\partial^2 y)=-(4\pi\sigma vM/c)\times[\sin\theta(d^2\theta/dx^2)+\cos\theta(d\theta/dx)^2]=f(x), \tag{2b}$$

$$\partial J_z/\partial x=(4\pi\sigma vM/c)(d\theta/dx)\cos\theta,$$

$$\partial J_z/\partial y=0. \tag{2c}$$

The necessary boundary conditions for the solution of Eqs. (2a)–(2c) are that all components of **J** vanish at large distances from the wall, J_y vanish at the film surfaces, and

$$(\partial J_x/\partial y)_{\text{film surfaces}}=(4\pi\sigma vM/c)(d\theta/dx)\times\sin\theta=h(x). \quad (3)$$

Equation (2a) was solved by introducing the Fourier transform for $J_x(x,y)$ with respect to x. The details of this solution are given in the Appendix.

$$J_x=\frac{1}{2\pi}\int_{-\infty}^{+\infty}\frac{\cosh(\zeta y)-\cosh\zeta(y-d)}{\zeta\sinh(\zeta d)}\times\int_{-\infty}^{-\infty}h(x')e^{-i\zeta x'}dx'e^{ix\zeta}d\zeta. \quad (4)$$

Equation (2b) was solved utilizing the usual Green's function techniques. The details of the solution are also given in the Appendix.

$$J_y=-\sum_{n\,\text{odd}}\frac{2d}{n^2\pi^2}\sin\left(\frac{n\pi y}{d}\right)\left[e^{-n\pi x/d}\int_{-\infty}^{x}f(x')e^{n\pi x'/d}dx'+e^{n\pi x/d}\int_{x}^{+\infty}f(x')e^{-n\pi x'/d}dx'\right]. \quad (5)$$

J_z can be obtained by direct integration.

$$J_z=(4\pi\sigma vM/c)\int_{-\infty}^{x}(d\theta/dx)\cos\theta dx. \quad (6)$$

This development has neglected the effect of the stray demagnetizing field $\mathbf{H}_s$ which is present when Bloch walls occur in thin films. If this field is included in a rigorous manner, solutions for **J** are not possible in simple form. However, for a linear wall, this field may be estimated using a model proposed by Néel[8] and developed by Middelhoek.[7] According to this model, the stray demagnetizing field is taken to be zero everywhere except within the wall where it has only a y component with value

$$H_s=-4\pi aM/\sqrt{2}(a+d). \quad (7)$$

This gives

$$dJ_z/dx=(4\pi\sigma vM/c)\{(d\theta/dx)\cos\theta-[a/\sqrt{2}(a+d)]\times[\delta(x+a/2)-\delta(x-a/2)]\}$$

or

$$J_z=\frac{4\pi\sigma vM}{c}\left[\int_{-\infty}^{x}\left(\frac{d\theta}{dx}\right)\cos\theta dx-\frac{a}{\sqrt{2}(a+d)}\right] \quad (8)$$

within the wall, while outside the wall $J_z=0$. Equations (4) and (5) are not affected.

[8] L. Néel, Compt. Rend. **241**, 533 (1955).

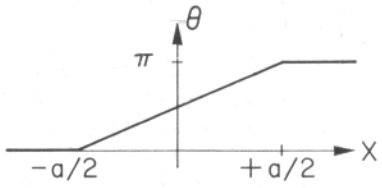

FIG. 2. Linear wall angle dependence. θ is the angle between **M** and $-z$ axis.

For the case of linear walls, the wall shape is $\theta=\pi(x/a+\frac{1}{2})$ for $|x|<a/2$, as shown in Fig. 2. With this functional form for $\theta(x)$,

$$h(x)=(4\pi\sigma vM/c)(\pi/a)\cos(\pi x/a), \quad |x|<a/2$$
$$h(x)=0, \quad |x|\geq a/2. \quad (9)$$

The x' integral Eq. (4) can be evaluated explicitly and the ζ integral can then be obtained in a straightforward manner by contour integration.

$$\frac{J_x}{J_0}=-\frac{1}{\pi}\sum_{n\,\text{odd}}\frac{2(-1)^n\cos(n\pi y/d)}{n(1+n^2a^2/d^2)}R_n(x), \quad (10)$$

$$R_n(x)=e^{-n\pi(|x|+a/2)/d}+e^{-n\pi(|x|-a/2)/d}, \quad \text{for} \quad |x|<a/2$$
$$R_n(x)=e^{-n\pi(|x|+a/2)/d}+e^{-n\pi(|x|-a/2)/d}, \quad \text{for} \quad |x|>a/2$$

where $J_0=4\pi\sigma vM/c$.

Using $f(x)=dh(x)/dx$ and Eq. (9), the integrals in Eq. (5) can be easily evaluated. Considering only $x>0$, the result is

$$\frac{J_y}{J_0}=-\frac{4}{\pi}\sum_{n\,\text{odd}}\frac{\sin(n\pi y/d)}{n(1+n^2a^2/d^2)}S_n(x), \quad (11)$$

$$S_n(x)=\sin(\pi x/a)-e^{-\frac{1}{2}n\pi a/d}\sinh(n\pi x/d), \quad \text{for } x<a/2$$
$$S_n(x)=e^{-n\pi x/d}\cosh(\tfrac{1}{2}n\pi a/d), \quad \text{for } x>a/2.$$

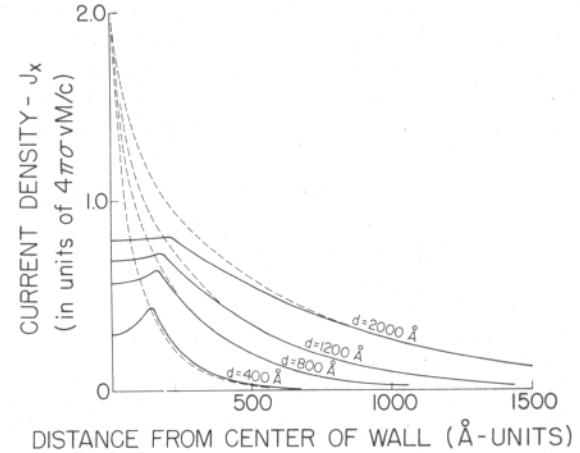

FIG. 3. Eddy current component J_x at the film surface ($y=0, d$) as a function of x (normal distance from wall center) with d (film thickness) as a parameter. Dotted curves represent the WSK results.

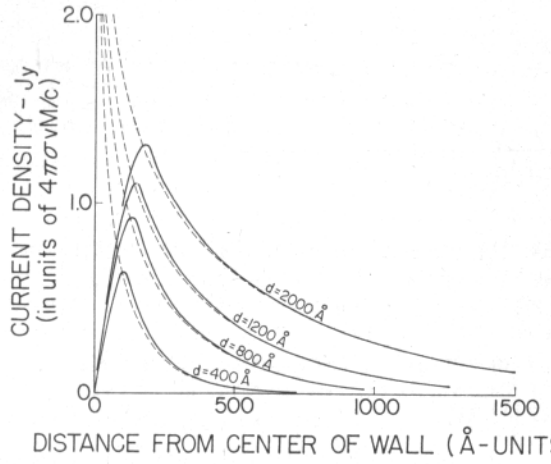

FIG. 4. Eddy current component J_y at the film center plane $y=d/2$, as a function of x (normal distance from wall center) with d (film thickness) as a parameter. Dotted curves represent the WSK results.

From Eq. (8), J_z becomes

$$\begin{aligned} J_z/J_0 &= \cos(\pi x/a) - a/\sqrt{2}(a+d), \quad \text{for} \quad |x| < a/2 \\ J_z/J_0 &= 0, \qquad\qquad\qquad\quad \text{for} \quad |x| > a/2. \end{aligned} \tag{12}$$

These solutions have been evaluated numerically with film thickness as a parameter. The wall width a was taken to have the thickness dependence calculated by Middelhoek.[7,9] Typical plots of the J_x, J_y, and J_z eddy current distributions are shown in Figs. 3–5, respectively. The current distributions exhibit maxima at x coordinates roughly corresponding to $a/2$, where a is the assumed Bloch wall width appropriate for each indicated film thickness. The current distribution clearly exhibits the effect of nonzero wall width. The original WSK calculation was made for wall motion in a long bar with rectangular cross section, and can be applied to thin films by allowing one of the dimensions to become arbitrarily large.[4] The results of the WSK calculation for this situation are also shown in Figs. 3–5. In the limit of small a/d, the present solutions reduce to those predicted by WSK. It must be pointed out that the present calculation is a valid approximation only when the x and z extensions of the material are much greater than d.

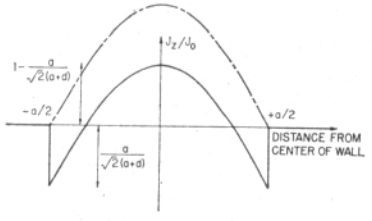

FIG. 5. Eddy current component J_z within the linear Bloch wall including demagnetizing field effects. The dashed curve corresponds to no demagnetizing-field effects. The WSK calculation yields $J_z=0$ everywhere.

[9] The material parameters used by Middelhoek are typical of Ni–Fe alloy (83% Ni) films deposited on 300°C substrates.

Taking a square path of integration in the x–y plane, centered at the origin with side length a, Stoke's theorem, Eqs. (1b) and (12) can be used to obtain $H \approx (\pi\sigma v a/c^2)(4\pi M)$. Using typical values, $a \approx 10^{-5}$ cm and $v \approx 10^4$ cm/sec, the result is that $H \approx 4\pi M \times 10^{-5}$. The assumption that $H \ll 4\pi M$ is reasonable. Further iteration will not significantly modify the **J** solution.

DOMAIN WALL MOBILITY

In terms of the current distribution, the eddy current losses per unit length of wall can be written as

$$W = (1/\sigma)\int J^2 dA \tag{13}$$

with integration over the x–y plane. Using the current distribution obtained in the previous section, W can be written

$$W = (4/\sigma)(4\pi\sigma v M/c)^2[I_{sq}(a,d) + I_{zsq}(a,d)], \tag{14a}$$

where

$$I_{sq}(a,d) = \frac{d^2}{\pi^3} \sum_{n \text{ odd}} \frac{A_n(R) + B_n(R)e^{-\pi R}}{n^3(1+R^2)^3} \tag{14b}$$

$$I_{zsq}(a,d) = (da/8)\{1 + [a/(a+d)]^2 - (8/\pi\sqrt{2})[a/(a+d)]\}, \tag{14c}$$

where $R = na/d$. In Eq. (14b), $A_n = 2 + \pi R - 2R^2 + \pi R^3$ and $B_n(R) = 2(1-R^2)$. Equation (14c) includes the stray demagnetizing field correction expressed in Eq. (12). If this correction is neglected, $I_{zsq}(a,d) = da/8$. In the limit $R \to 0$, Eq. (14) reduces to the loss expression calculated by WSK. For a 180° domain wall moving with a velocity v in an easy-axis field H, the rate of energy loss for the system (the two domains and the moving wall) is $2dvMH$. By equating the eddy current losses to the system loss, the eddy-current-limited mobility can be obtained.

$$G_e = \partial v/\partial H = dc^2/32\pi^2\sigma M[I_{sq}(a,d) + I_{zsq}(a,d)]. \tag{15}$$

The mobilities obtained from the present calculation are shown in Fig. 6 as a function of film thickness. The resistivity was taken to be 20 $\mu\Omega\cdot$cm, corresponding to

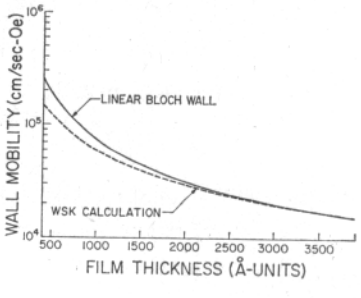

FIG. 6. Eddy-current-limited wall mobility as a function of film thickness, calculated using linear Bloch walls and walls widths determined from static energy considerations.

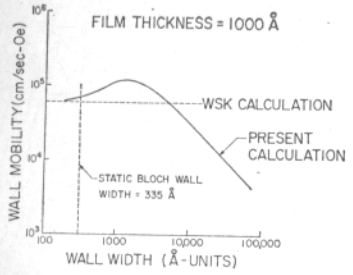

FIG. 7. Eddy-current-limited wall mobility as a function of domain wall width for 1000-Å film thickness.

$\sigma=0.45\times10^{17}$ sec^{-1} in Gaussian units, which is typical for the Ni–Fe alloy films investigated.[9] The curve in Fig. 6 includes the stray demagnetizing field correction expressed in Eq. (14c). The WSK mobility is plotted in the same figure. In the present calculation, the losses due to J_x and J_y are less than predicted by WSK. However, the additional losses due to J_z (J_z is zero for WSK) partially compensate for the reduced losses due to J_x and J_y. If the stray demagnetizing field correction is neglected the losses due to J_z almost exactly compensate for the reduced losses due to J_x and J_y, resulting in mobilities which are even closer to the WSK predictions. In any case, the correction to the mobility due to the stray demagnetizing field is small. Further refinement of this correction would be pointless. The present calculation yields mobilities which are not significantly different from the WSK calculation, even though the actual current distributions clearly show the effect of finite wall width. As discussed earlier, the most recent mobility measurements are almost an order of magnitude lower than these calculated values.

Recently, a different type of wall structure has been observed in thin films by Torok.[10] This type of wall consists of alternating Bloch wall sections separated by Bloch lines. If the stray-field energy is reduced by this alternation, the domain wall may be much wider than expected for Bloch walls. In Fig. 7, the eddy-current-limited wall mobility for 1000-Å-thick films is shown as a function of wall width. For sufficiently wide walls, the $I_{zsq}(a,d)$ loss term dominates, and the mobility is significantly smaller than expected from either the WSK calculation or the present calculation assuming Bloch walls.

It therefore appears that eddy current losses in thin ferromagnetic films, calculated on the basis of static Bloch wall shapes, do not provide an adequate explanation of the mobility data. If the actual wall structures performing the motion are significantly wider than static Bloch walls, the present calculation predicts increased eddy current losses and mobilities more consistent with recent mobility data. Otherwise, some other loss mechanism must dominate.

[10] E. J. Torok, A. L. Olson, and H. N. Oredson, J. Appl. Phys. 36, 1394 (1965).

APPENDIX

Solution for J_x: It is necessary to solve Eq. (2a) subject to two boundary conditions, one given by Eq. (3), and the other that J_x vanishes at $x=\pm\infty$. Since the range of the variable is $\pm\infty$ and the function vanishes at these limits, one can make use of Fourier transforms. Taking the Fourier transform of Eq. (2a) with respect to x, one obtains

$$[\partial^2\bar{J}_x(\zeta,y)/\partial y^2]-\zeta^2\bar{J}_x(\zeta,y)=0. \tag{16}$$

Eq. (16) has a solution of the form

$$\bar{J}_x=A(\zeta)^{-\zeta y}+B(\zeta)e^{\zeta y}, \tag{17}$$

where $A(\zeta)$ and $B(\zeta)$ are arbitrary functions of ζ.

Applying the boundary condition in Eq. (3), and solving for $A(\zeta)$ and $B(\zeta)$, one obtains

$$A(\zeta)=-\bar{h}(\zeta)(e^{\zeta d}-1)/2\zeta\sinh(\zeta d) \tag{18}$$

and

$$B(\zeta)=-\bar{h}(\zeta)(e^{-\zeta d}-1)/2\zeta\sinh(\zeta d), \tag{19}$$

where

$$\bar{h}(\zeta)=\int_{-\infty}^{+\infty}h(x')e^{i\zeta x'}dx'.$$

Eq. (3) is obtained by taking the inverse transform of $\bar{J}_x(\zeta,y)$.

Solution for J_y: It is necessary to solve Eq. (2b) subject to the boundary conditions that $\bar{J}_y$ vanishes at $y=0$, $y=d$, and $x=\pm\infty$. A common technique of solving inhomogeneous partial differential equations is to obtain the Green's function which satisfies the equation

$$(\partial^2\Omega/\partial x^2)+(\partial^2\Omega/\partial y^2)=\delta(x-x') \tag{20}$$

subject to the given boundary conditions.

The solution is

$$\Omega(x,x',y)=\begin{cases}\displaystyle\sum_{n\,\text{odd}}-\frac{2d}{n^2\pi^2}e^{-n\pi x'/d}e^{n\pi x/d}\sin\left(\frac{n\pi y}{s}\right) & \text{for } x<x'\\ \displaystyle\sum_{n\,\text{odd}}-\frac{2d}{n^2\pi^2}e^{n\pi x'/d}e^{-n\pi x/d}\sin\left(\frac{n\pi y}{d}\right) & \text{for } x>x'.\end{cases} \tag{21}$$

Consequently, one obtains the solution to Eq. (2b).

$$J_y(x,y)=\int_{-\infty}^{+\infty}f(x')\Omega(x,x'y)dx'. \tag{22}$$

Eq. (5) is obtained by substituting Eq. (21) into Eq. (22).

Reprinted from JOURNAL OF APPLIED PHYSICS, Vol. 37, No. 11, 4301, October 1966
Copyright 1966 by the American Institute of Physics
Printed in U. S. A.

Erratum: Eddy-Current-Limited Domain-Wall Motion in Thin Ferromagnetic Films

[37, 3594 (1966)]

CARL E. PATTON, THOMAS C. MCGILL, AND CHARLES H. WILTS
California Institute of Technology, Pasadena, California

THE current distribution should be corrected as follows:

$$\frac{J_x}{J_o}=F(x,y)-\frac{4}{\pi}\sum_{n\,\text{odd}}\frac{\cos(n\pi y/d)}{n(1+n^2a^2/d^2)}Q_n(x) \qquad (10)$$

$$F(x,y)=\frac{\cosh(\pi y/a)-\cosh[\pi(y-d)/a]}{\sinh(\pi d/a)} \qquad 0<x<a/2,$$

$$Q_n(x)=\cosh(n\pi x/d)e^{-n\pi a/2d} \qquad 0<x<a/2,$$

$$F(x,y)=0 \qquad x>a/2,$$

$$Q_n(x)=\cosh(n\pi a/2d)e^{-n\pi x/d} \qquad x>a/2.$$

A negative sign should precede the expression for J_y in Eq. (11). The current distributions for J_x and J_y in Figs. 3 and 4 are incorrect. Correct Figs. 3′ and 4′ are shown here. In the loss calculation, Eq. (14b) should be corrected as follows:

$$I_{sq}(a,d)=\frac{d^2}{\pi^3}\sum_{n\,\text{odd}}\frac{\pi R_n(1+R_n^2)+2(1+e^{-\pi R_n})}{n^3(1+R_n^2)^2}, \qquad (14b)$$

where $R_n=na/d$. The first complete sentence after Eq. (14c) should be deleted. The correct mobility for Fig. 6 is shown here in Fig. 6′. For very thin films (thickness less than 1000 Å) the mobility is slightly greater than predicted by WSK. For thicker films, the additional losses due to J_z yield a mobility which is slightly lower than predicted by WSK.

It has been pointed out by F. B. Hagedorn that a more realistic representation of the stray field may be obtained by multiplying the right-hand side of Eq. (7) by $\sqrt{2}\sin\theta$. This modification will remove the discontinuity in the J_z distribution of Eq. (12). The dotted curve of Fig. 5 is the correct current distribution (including stray field effects) if the amplitude is changed from unity to $d/(a+d)$. This modification does not appreciably change the mobility plot shown in Fig. 6′. With this modification, however, I_{zsq} will tend to zero for large wall width ($a \gg d$). Because of this the mobility will monotonically increase with increasing wall width, for a fixed film thickness. This improved treatment of the demagnetizing field indicates that Fig. 7 is incorrect for wall widths greater than 1000 Å. Large wall widths will not result in a reduced mobility.

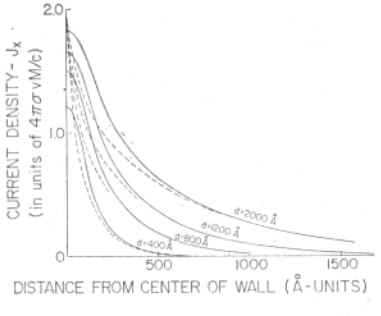

FIG. 3′. Corrected eddy-current component J_x at the film surface ($y=0,d$) as a function of x (normal distance from wall center) with d (film thickness) as a parameter. Dotted curves represent the WSK results.

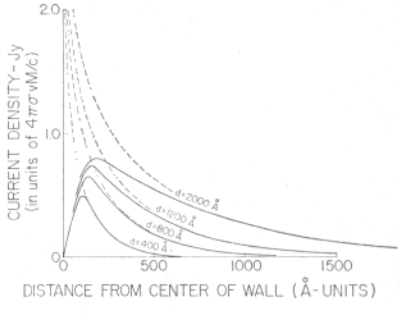

FIG. 4′. Corrected eddy-current component J_y at the film center plane $y=d/2$, as a function of x (normal distance from wall center) with d (film thickness) as a parameter. Dotted curves represent the WSK results.

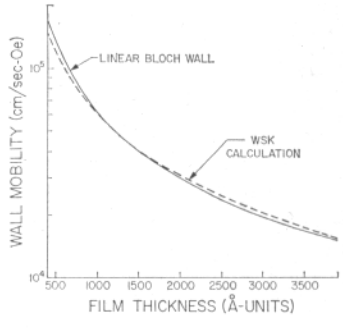

FIG. 6′. Corrected eddy-current-limited wall mobility as a function of film thickness, calculated using linear Bloch walls and wall widths determined from static energy considerations.